Optics Communications 428 (2018) 176–181

Contents lists available at ScienceDirect

Optics Communications

journal homepage: www.elsevier.com/locate/optcom

# Spectral domain optical coherence tomography using an optical wavefront splitting interferometer

Yimin Wang [a,*], Xiaobing Chen [b], Tianran Yuan [a], Qiankun Zhang [a], Linna Zhang [a]

[a] Department of Mechanical and Material Engineering, Huaiyin Institute of Technology , East Meicheng Road, No. 1, Huaian, 223003, China
[b] Department of Computer Engineering, Huaiyin Institute of Technology, East Meicheng Road, No. 1, Huaian, 223003, China

ARTICLE INFO

*Keywords:*
Optical coherence tomography
Medical and biological imaging
Rayleigh interferometer

ABSTRACT

Coherence-domain ranging in optical coherence tomography (OCT) is usually performed using a Michelson interferometer. In this study, a spectrometer based OCT system with a wavefront splitting interferometer is investigated. Instead of using a transmission beam splitting mirror or fiber optic coupler, a silver coated mirror is used to split a portion of the OCT source light into the reference arm of the interferometer. Reference and backscattered sample light of the OCT system interfere non-collinearly in the wavefront splitting interferometer. The OCT system is polarization insensitive, and beam splitting ratio between sample and reference arms is adjustable through controlling the insertion of the beam reflector. Biological tissues are imaged successfully using our OCT setup. This study demonstrates that a non-collinear optical interferometer is also good to be used for OCT imaging.

## 1. Introduction

Optical coherence tomography (OCT) [1] can be used to perform noninvasive sectional imaging of transparent as well as turbid biological tissues. Through measuring singly backscattered light as a function of depth, OCT provides tissue structure with high resolution and sensitivity *in vivo*. OCT has become a widely used imaging method in the diagnosis of retinal diseases [2,3]. In addition to obtain morphological images, OCT can also detect a Doppler frequency shift of reflected light, which provides information on blood flow [4,5]. Through analyzing the polarization state change of sample reflections, polarization sensitive OCT is used to evaluate the severity of tissue degradation [6–8]. Catheter-based OCT probes have been developed to extend the OCT application for endoscopic imaging of internal organs [9–11]. OCT probes built in cardiology study have shown promise for intracoronary imaging and can be used to visualize clinically important coronary plaque microstructures [12].

Coherence-domain ranging in OCT is usually performed using a Michelson interferometer (MI), which belongs to optical amplitude splitting technique. In a MI based spectral domain OCT (SD-OCT) system [13,14], light from a low coherence source is launched into the source arm of the interferometer, which consisting of a 2X2 optical beam splitter. The optical coupler splits the source light between the reference and sample arms. The reflected reference and back scattered sample light are recombined at the coupler, and then the interference signal enters a spectrometer. Mach–Zehnder interferometer is another type of optical amplitude splitting interferometer which is employed for balanced detection in swept source OCT [15].

Besides optical amplitude splitting method, wavefront splitting is also an important technique used in the optical interference study, such as the Rayleigh interferometer (RI) which measures the interference pattern produced by two parallel coherent light beams [16–18]. In OCT study, wavefront splitting method has ever been used to generate multiple OCT images encoded at different imaging depth [19,20]. For example, in C. Pedersen's paper [19], wavefront of the probe beam is divided into two parts by a glass plate to form dual beam illumination at the sample. But in those studies, the OCT system is still based on a MI interferometer. The purpose of this paper is to present our investigation about the application of a wavefront splitting interferometer for OCT imaging. In our experiment, reference and sample beams interfere non-collinearly in the SD-OCT system. Biological tissues are imaged successfully using our OCT setup.

## 2. Methods

### 2.1. Experimental setup

The SD-OCT system employed in this study is schematically illustrated in Fig. 1. It contains a power adjustable superluminescent diode

* Correspondence to: Department of Mechanical and Material Engineering, Huaiyin Institute of Technology, East Meicheng Road, No. 1, 14-208, Huaian, 223003, China.
*E-mail address:* ywang12345@126.com (Y. Wang).

https://doi.org/10.1016/j.optcom.2018.07.060
Received 1 May 2018; Received in revised form 17 July 2018; Accepted 21 July 2018
Available online 26 July 2018

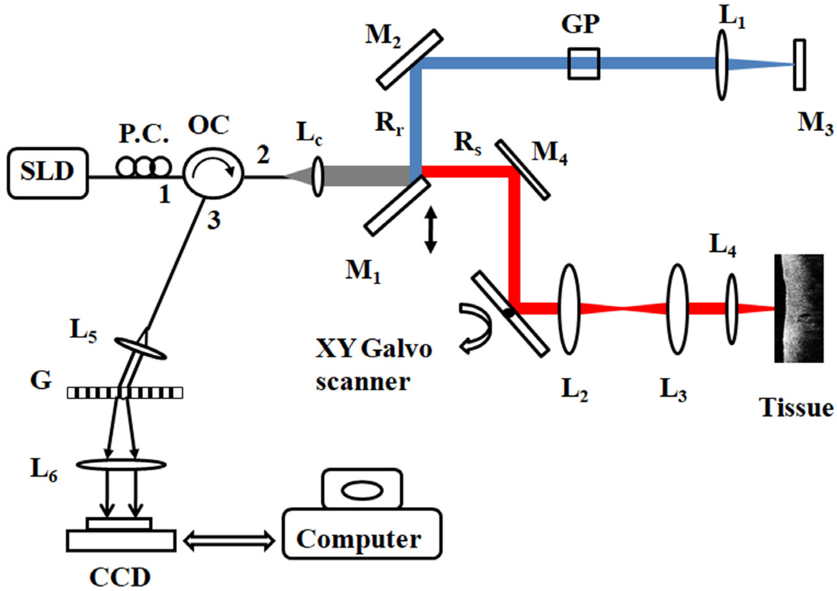


**Fig. 1.** SD-OCT setup with a wavefront splitting interferometer.

(SLD) source with a center wavelength of 850 nm and a bandwidth of 33 nm. Light from the SLD travels through a fiber optic circulator OC from its port 1 to 2, and then enters the interferometer with power $P_0$. A portion of the source light (power $P_r$) emerging from the collimation lens $L_c$ is reflected into the reference arm of the interferometer (shown as the blue line) by a silver coated mirror $M_1$, and the other portion (power $P_s$) travels directly into the sample arm, shown as the red line. Thus, wavefront of the light emerging from lens $L_c$ is divided into two parts by the beam reflector $M_1$. Splitting ratio R between sample and reference beams is $R = R_s/R_r$, in which $R_s = P_s/P_0$, $R_r = P_r/P_0$, and $R_s + R_r = 1.0$.

The reference arm consists of a silver coated mirror $M_2$, a K9 glass plate GP for dispersion compensation, and a lens $L_1$ which focuses light onto the silver coated mirror $M_3$. The sample arm consists of a pair of galvanometers for 2-axis beam steering, two f = 40 mm scan lenses $L_2$ and $L_3$, and a f = 30 mm objective lens $L_4$ which focusing probe beam onto the sample. The probe beam should be aligned along the optical axis of the sample arm. Reflected reference and backscattered sample light, collected by lens $L_c$, enter the port 2 of the optical circulator, as shown in Fig. 2, where $E_s$ and $E_r$ represent sample and reference light separately. It can be seen that the sample and reference light travel non-collinearly. Basic structure of the interferometer in Fig. 1 is a modified RI interferometer, in which port 2 of the optic circulator serves as the source and detection port of the RI interferometer.

In Fig. 1, the composite signal output from port 3 of the circulator OC is detected by a custom spectrometer. The spectrometer consists of a f = 60 mm collimating lens $L_5$, a diffraction grating G (1200 lp/mm), an IR achromatic doublet lens $L_6$ (f = 150 mm), and a 2048 element CCD line scan camera. The camera has a 12-bit resolution. The spectrum, which contains the encoded depth reflectivity information, is measured by the CCD camera. The exposure time of the camera is set as 100 μs in this study. Data from the camera are transferred via the Cameralink interface to a computer. A VC++ program running on the computer coordinates the frame grabber and galvanometers, and provides data acquisition, processing, and image displaying.

In the OCT interferometer, sample and reference beams travel non-collinearly and combine at the entrance of the circulator OC, as shown in Fig. 2. Optical path difference $\Delta$ between sample and reference light can be expressed as

$$\Delta = \sum^{p} n_j l_j - \sum^{q} n_m l_m \tag{1}$$

where $l_j$ is the length of the $j$th optical element (including air space) in the sample arm with refractive index $n_j$, and $l_m$ is the length of the $m$th optical element in the reference arm with refractive index $n_m$. At the point where beams from sample and reference arms combine together, light field will be changed in accordance with the variation of optical path difference $\Delta$, and reach the maximum at $\Delta = 0$. The interference signal should not be affected by the angle between two focusing beams $E_s$ and $E_r$ at the entrance of the circulator, because the path difference $\Delta$ is independent of that angle in accordance with Eq. (1).

### 2.2. Variable beam splitting ratio

In Fig. 1, a small portion of the collimated source light is reflected into the reference arm by mirror $M_1$. For a Gaussian beam with power $P_0$, light intensity I(r) in the beam cross section can be expressed as: $I(r) = I_0 \exp(-2r^2/\omega^2)$, in which $I_0$ is the light intensity at the beam center, r is the radial coordinate of the beam, and $\omega$ is the beam radius where the light intensity is $1/e^2$ of that at the beam center. If the beam is blocked by a reflector with its edge at the position $x_1$, as shown in Fig. 3, ratio $\beta$ between the transmitted light power $P(x_1)$ and input power $P_0$ can be expressed as:

$$\begin{aligned} \beta &= P(x_1)/P_0 \\ &= \int_{-\infty}^{\infty}\int_{x_1}^{\infty} I(x,y)dxdy \Big/ \int_{-\infty}^{\infty}\int_{-\infty}^{\infty} I(x,y)dxdy \\ &= \frac{1}{2} - \frac{1}{\sqrt{\pi}}\int_0^{\sqrt{2}k} e^{-x^2}dx \end{aligned} \tag{2}$$

in which k ($k = x_1/\omega$, or $x_1 = k\omega$) is a factor representing the insertion depth of the mirror. Then, beam splitting ratio R between sample and reference arm is

$$R = \beta/(1-\beta) \tag{3}$$

Fig. 4 shows the calculated beam splitting ratio R at different k using Eqs. (2) and (3). It can be seen that, for the interferometer in Fig. 1, beam splitting ratio between its sample and reference arm is adjustable. It can be tuned continuously through controlling the insertion of mirror $M_1$ in the beam path of the collimated source light. When k = 0, $x_1$ is equal to 0 and half of the source light is reflected by mirror $M_1$. So the beam splitting ratio R is equal to 1.0, shown as the black dot in Fig. 4.